

# Enhancement of emission currents in plasma electron sources based on a low-pressure arc discharge

T V Koval<sup>1,a</sup>, V N Devyatkov<sup>2,b</sup> and Nguyen Bao Hung<sup>1,c</sup>

<sup>1</sup> National Research Tomsk Polytechnic University, 30 Lenin Ave., Tomsk, 634050, Russian Federation

<sup>2</sup> Institute of High Current Electronics SB RAS, 2/3 Akademicheskoy Ave., Tomsk, 634055, Russian Federation

E-mail: <sup>a</sup> tvkoval@mail.ru, <sup>b</sup> vlad@opee.hcei.tsc.ru, <sup>c</sup> baohung.ng@gmail.com

**Abstract.** The paper reports on a theoretical and experimental study of the discharge plasma generation with an enhanced electron emission current in a plasma electron source based on a low-pressure arc discharge with a grid-stabilized plasma emission boundary. The source operates at a pressure in the working chamber of  $p = 0.02\text{--}0.05$  Pa (Ar), accelerating voltage of up to  $U_a = 10$  kV, and longitudinal magnetic field for electron beam transport of up to  $B_z = 0.1$  T. The experiments show that in the mode of electron emission from the plasma, the voltage  $U_d$  between the cathode and grid electrode changes its sign. The numerical simulation demonstrates that the plasma potential and voltage  $U_d$  depend on the electric field penetrating from the acceleration gap into the discharge region through the grid meshes, and on the discharge current, gas pressure, geometric transparency of the grid, and gas kind. It is shown that the main mechanisms responsible for the increase in the discharge current and electron emission current from the plasma are associated with secondary ion-electron emission from the emission electrode and with positive feedback between the region of cathode plasma generation and the channel of electron beam transport.

## 1. Introduction

Plasma electron sources with a grid-stabilized plasma emission boundary provide stable generation of emission plasma and electron beams with a high current density of  $j_b = 1\text{--}10$  A/cm<sup>2</sup> [1–4]. In these sources, the electrons are emitted from a partially open plasma surface in the central part of the grid meshes and through a potential barrier at their edges. The electron emission from the plasma can not only change its potential but also affect the other parameters of the plasma, resulting in an unstable discharge and high-frequency oscillations [5, 6], in a change of the plasma density and attendant growth of the discharge current. The processes occurring in the region of the emission grid electrode should be taken into account in designing of both plasma emitters and their power supplies. Understanding these processes will allow one to define more accurately the requirements on the parameters of power supplies and to determine the methods that enhance the operation stability of plasma cathodes with a grid-stabilized plasma emission boundary and increase their limiting parameters.

The paper studies the effect of a positive feedback between the discharge region and plasma anode on the generation of plasma and electron beam, discharge current, and electron beam current. The dependence of the plasma potential and voltage between the cathode and emission electrode on the discharge current and gas pressure is investigated. The mode in which electron extraction from the



plasma cathode provides much higher amplitudes of the beam and discharge currents compared to those with no electron extraction is considered.

## 2. Plasma electron source

The experimental electron source based on a grid plasma cathode is described elsewhere [7]. A simplified schematic of the source is shown on figure 1. The discharge system of the plasma cathode is partially placed in a divergent magnetic field of solenoid 7; in the emission grid region,  $B_g = 25\text{--}35$  mT. The electron beam is extracted through an emission window of diameter 60 mm covered with a stainless steel grid shaped to a mesh size of  $0.3 \times 0.3$  mm and is transported in drift tube 4 of diameter 80 mm to collector 5 spaced by 250 mm from grid electrode 3. The diameter of anode 2 is 80 mm, and its length is 70 mm. Of significance in the electron source is the interrelation between the processes occurring in the plasma anode, which is formed in the beam drift space during ionization of the working gas, and the processes developing in the plasma cathode due to secondary ion-electron emission from the surface of grid electrode 3 [7–9].

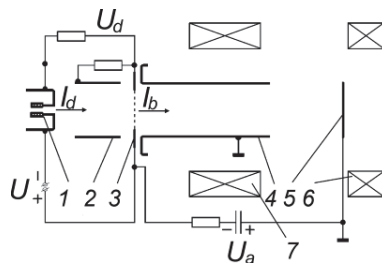


**Figure 1.** Electrodes of the plasma-cathode electron source: 1 – cathode, 2 – anode, 3 – grid electrode, 4 – drift tube, 5 – collector, 6, 7 – solenoids.

Figure 2 presents typical waveforms of the discharge current  $I_d$  and voltage  $U_d$  between electrodes 1 and 3 in the mode with no electron emission (accelerating voltage  $U_a = 0$ ). In this mode, almost the whole discharge current takes the path through grid electrode 3. The voltage  $U_d$  measured in the discharge gap at  $p = 0.07$  Pa varies in the range from 20 to 70 V for the discharge current  $I_d$  ranging from 80 to 280 A. Typical waveforms of the discharge current  $I_d$ , beam current  $I_b$ , and voltage  $U_d$  in the mode with electron emission at  $U_a = 10$  kV are presented in figure 3. Figure 4 shows the voltage  $U_d$  depending on the gas pressure (in the plasma anode) for the modes with no electron emission (curves 3, 4) and with electron emission (curves 1, 2) at a discharge current of 150 and 250 A.

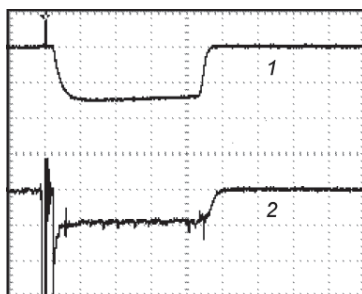


**Figure 2.** Typical waveforms of the discharge current  $I_d$  (1) and voltage  $U_d$  (2) at  $B_g = 25$  mT,  $p = 0.1$  Pa,  $U_a = 0$ . Scale: 100 A/div, 50  $\mu$ s/div, 40 V/div.

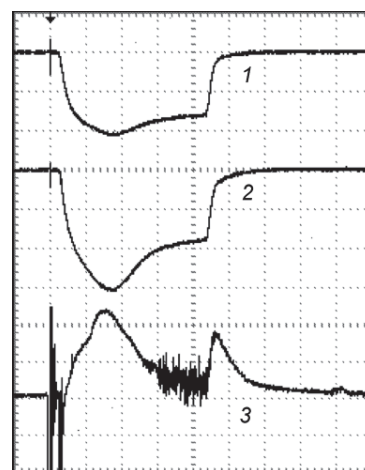


**Figure 3.** Typical waveforms of the currents  $I_d$  (1),  $I_b$  (2), and voltage  $U_d$  (3) at  $B_g = 25$  mT,  $p = 0.1$  Pa,  $U_a = 10$  kV. Scale: 100 A/div, 50  $\mu$ s/div, 40 V/div.

### 3. Discharge plasma characteristics

The characteristics of the discharge plasma in the electrode system of the plasma cathode were studied using a numerical drift-diffusion model. Figure 5 illustrates the mode with no electron emission, showing the plasma density distribution in an inhomogeneous magnetic field at a gas pressure of 0.1 Pa (argon) in the discharge region; the magnetic field at the grid edge is 25 mT. It is seen that the plasma density distribution is nonuniform, and this is responsible for the radially nonuniform distribution of the beam current density.

Figure 6 shows the plasma density  $n_e$  and plasma potential  $\phi$  depending on the gas pressure in the central region of the emission grid at a discharge current of 150 and 250 A. The plasma temperature  $T_e$  at a current of 150 A decreased from 18 to 10 eV with increasing the pressure from 0.05 to 0.2 Pa. The calculations take into account that the pressure in the plasma cathode is 1.5–2 times higher than that downstream of its emission grid in the beam transport region.

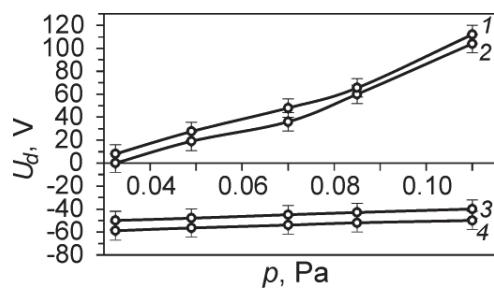


**Figure 4.** Voltage  $U_d$  vs the pressure  $p$  in the emission grid region:  $U_a = 10$  kV (1, 2);  $U_a = 0$  (3, 4);  $I_d = 250$  A (1, 4);  $I_d = 150$  A (2, 3);  $B_g = 25$  mT.

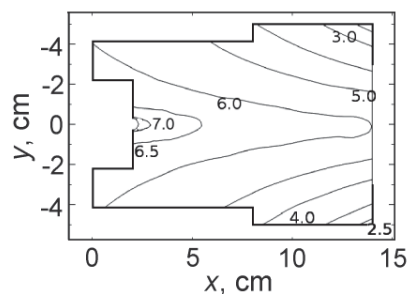


**Figure 5.** Plasma density distribution in the electrode system ( $10^{11} \text{cm}^{-3}$ ) of the plasma cathode.

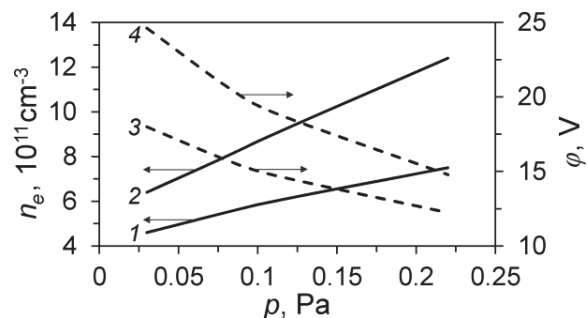


**Figure 6.** Plasma density  $n_e$  (1, 2) and plasma potential  $\phi$  (3, 4) vs the gas pressure (argon) at  $I_d = 150$  A (1, 3) and  $I_d = 250$  A (2, 4)

### 4. Mathematical model

Let us consider the physical mechanisms responsible for the dependences of the voltage  $U_d$  on the gas pressure  $p$  and discharge current  $I_d$  (figure 4), taking into account the secondary processes at the cathode, in the discharge region of the hollow cathode, and at the emission electrode. The ion current in the plasma anode and the electron current to the hollow cathode are negligible and ignored. The discharge currents at the cathode, to the emission electrode, and in the acceleration gap are written as

$$I_d = I_{em} + I_{\sigma c} + I_i, \quad (1)$$

$$I_d = I_{eb} + j_{ch} S_e (1 - l_i / r_0)^2 + I_i, \quad (2)$$

$$I_b = I_{em} + I_{\sigma a} + I_{ia} \quad (3)$$

Here  $S_e = \pi r_0^2$  is the area of a grid mesh;  $S_e(1 - l_i / r_0)^2$  is the electron emission area;  $I_{eb}$  is the current of fast electrons that not involved in ionization;  $j_{ch}$  is the chaotic electron current density;  $I_{\sigma, a}$  is the secondary electron current;  $I_i$  is the ion current transported from the acceleration gap to the discharge

region through the meshes of the emission electrode;  $I_{ia}$  is the ion current in the plasma anode;  $l_i$  is the layer width separating the plasma from the grid:  $l_i = (4\pi n_{ic})^{-1/2} \varphi^{3/4} (ekTe)^{-1/4}$ ;  $n_{ic}$  is the discharge plasma density with regard to its local increase due to bombardment of ions arrived from the acceleration gap [4];  $\varphi$  is the potential fall across the layer  $l_i$ . The plasma density is determined for the equilibrium state from the equation of balance between the rate of charged particle loss and the ionization rate [10, 11]. The system of equations (1)–(3) contains a feedback through the currents in the discharge region and plasma anode.

In the mode with no electron emission, the potential difference between electrodes 1 and 3 (figure 1) is  $U_d = -|U_c| + \varphi$ , where  $U_c$  is the voltage in the near-cathode layer of the space charge, and the plasma potential is  $e\varphi/kT_e = \ln[j_{ch}S_e/I_d]$ , where  $S_e$  is the emission electrode area. In the mode with electron emission,  $\varphi = DU$ , where

$$\varphi = mc^2 \left[ \frac{4\sqrt{2\pi}I_d}{NI_A} \right]^{2/3} \left[ \left( \frac{j_{ch}S_e}{I_d} \right)^{1/2} - 1 \right]^{3/4}, \quad DU = r_0c_1 \frac{U_a}{d(t)} \exp\left( -c_2 \frac{\rho - z}{r_0} \right) \quad (4)$$

The potential  $\varphi$  is determined from the condition of current continuity in the plasma cathode in the mode of emission from the open plasma surface. The potential  $U$  characterizes the acceleration gap field penetrating into the grid meshes to a certain depth  $z$ . The acceleration gap width is determined according to the 3/2 power law:  $d(t) = (\sqrt{2/9\pi})^{1/2} \left[ U_a^{3/2}/j_b(t) \right]^{1/2}$ ;  $I_A = 17$  kA;  $D$  is the dielectric constant of the emission electrode;  $N$  is the ratio between the grid area and the area of a grid mesh; for the grid with a mesh size of  $0.3 \times 0.3$  mm and wire thickness of  $\rho = 0.15$  mm, the coefficients are  $c_1 = 0.3$ ,  $c_2 = 0.44$ ;  $z = 0$  is the grid plane from the side of the discharge plasma.

The stationary position of the electron-emitting plasma surface  $z_{pl}$  adjacent to the region of the electric field is determined by the condition of equality between the gas-kinetic pressure of the plasma  $8\pi kT_e n_i$  and pressure of the electrostatic field  $E^2$ . A change of the extracting voltage or plasma density causes displacement of the boundary of the emitting plasma surface  $z_{pl}$ .

A decrease in the layer thickness  $l_i$ , i.e., an increase in the emission surface area  $S_e(1-l_i/r_0)^2$ , breaks the condition necessary for electron acceleration: maximum electron emission current (2) in the acceleration gap may not exceed discharge current (1). The discharge current is cut off due to the processes occurring inside the discharge region. As the discharge current is switched to the acceleration gap, the voltage across the gap drops steeply and the plasma potential decreases. In experiments reported elsewhere [7], the current cutoffs were followed by reignition of the discharge with recovery of its amplitude. This is possible when the gas-kinetic pressure of the discharge plasma reaches the pressure of the accelerating electric field.

The coefficient of electron extraction from the plasma cathode is determined as the ratio of beam current (3) in the acceleration gap to the discharge current  $\alpha = I_b/I_d$ :

$$\alpha = 1 + (1 + \gamma_a) \frac{I_{ia}}{I_d} = 1 + (1 + \gamma_a) F(p, \gamma_a), \quad (5)$$

where the function  $F$  is obtained by solving the current continuity and ion balance equations [10],  $\gamma_a$  is the ion-electron emission coefficient. The extraction coefficient  $\alpha$  larger than unity is mainly due to the processes in the plasma anode that provide amplification of the beam current through ion-electron emission from the surface of the emission electrode. The coefficient  $\alpha$  depends heavily on the gas pressure  $p$ , guide magnetic field, accelerating voltage, and also on the material and surface smoothness of the emission grid electrode.

## 5. Numerical estimates

The voltage between cathode 1 and grid electrode 3 (figure 1) in the mode of electrons emission is  $U_d = -|U_c| + U_f + \varphi$ , where  $U_f$  is the potential of the accelerating field between the face of the drift tube and emission electrode (figure 1). Figure 7 shows calculated dependences of the voltage  $U_d$  on the gas pressure (argon) in the mode with no electron emission (3, 4) and with electron emission (1, 2). For the mode with no electron emission (curves 3, 4), the dependences were calculated using the values of the plasma density and temperature in figure 6.

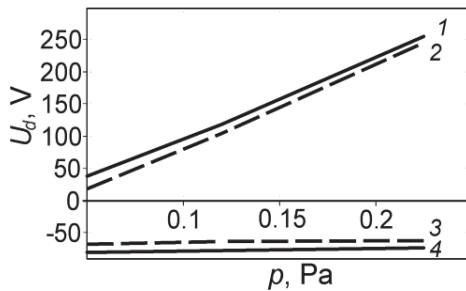


**Figure 7.** Calculated dependences of the voltage  $U_d$  on the pressure  $p$  (in the emission grid region):  $U_a = 10$  kV (1, 2),  $U_a = 0$  (3, 4),  $I_d = 250$  A (1, 4),  $I_d = 150$  A (2, 3).

The dependences of the voltage  $U_d$  for the mode with electron emission (figure 7, curves 1, 2) were calculated by formula (4). The polarity reversal of the voltage  $U_d$  in this mode (figure 4 and figure 7) owes to the influence of the accelerating field on the formation of the positive charge layer in the region of emission holes. The rather strong pressure dependence of  $U_d$  is due to the dependence of the plasma potential  $\varphi$  on the plasma density that increases almost linearly with increasing gas pressure.

Increasing the discharge current  $I_d$  from 150 to 250 A causes the voltage  $U_d$  to increase almost steadily over the entire pressure range (figure 4 and figure 7). From this, it follows that the emission current varies with  $I_d$  mainly due to fast electrons that take the path through the grid meshes to the acceleration gap.

The pulse shape of the beam current is defined in many respects by the processes in the plasma anode. Moreover, the rate of gas ionization during the rise time of the discharge current is higher due to the difference in the rates of supply of fast electrons, generation and loss of plasma particles. The time dependence of the voltage  $U_d$  (figure 3), as is seen from relation (4), is defined by the pulse shape of the beam current. In the experiment considered, the discharge and emission currents grow simultaneously due to the positive feedback (figure 3). At the peaks, the relative change of the discharge and emission currents is 1.4–1.5, and as the pulses are flattened, it is 1.2.

As has been shown [12], the pulse shape and amplitude of the beam current  $I_b$  depend heavily on the grid material and plane part of the emission electrode, gas kind, and operating mode of the plasma anode: for plasma electrons, the rate of residual gas ionization in the drift space increases in the mode of a reflex discharge [13]. In experiments on the SOLO electron source with a plasma cathode and grid stabilization, the total emission current (with a rectangular pulse shape) was increased up to 2 times without any apparent variation in the discharge current at a magnetic field of 3.6–30 mT and gas (Ar) pressure of 0.015–0.04 Pa. In the experiments reported in the present paper, the discharge current reveals an increase at  $p = 0.1$  Pa (figure 3). Increasing the pressure and the magnetic field increases the effect of the feedback on the discharge current due to the ion current from the acceleration gap and to the ions arrived from the discharge region of the cathode to the potential well at the grid surface.

## 6. Conclusion

Thus, we considered the theoretical model that describes the dependence of the grid electrode potential with respect to the plasma on the parameters of the system with enhanced emission currents. The experimental and calculated dependences show a qualitative agreement, suggesting that the electrons are emitted from the partially open plasma surface in the central part of the emission holes.

The polarity reversal of the voltage  $U_d$  in the mode of electron emission owes to the effect of the accelerating field on the formation of the positive charge layer in the region of the emission holes. The voltage  $U_d$  depends heavily on the gas pressure and hence on the discharge plasma density.

The processes in the plasma anode that are associated with the rates of bulk gas ionization by the electron beam and ion-electron emission at the emission electrode define the amplitude and pulse shape of the beam current and discharge current. The positive feedback can provide a simultaneous increase in the discharge and emission currents.

### Acknowledgement

The experimental part of the work was supported by the Russian Science Foundation (project No. 14-29-00091).

### References

- [1] Kreindel Yu E 1977 *Plasma Electron Sources* (Moscow, Atomizdat) (in Russian)
- [2] Zharinov A V, Kovalenko Yu A, Roganov I S, Tyuryukanov P M 1986 Plasma electron emitter with grid stabilization *Zh. Tekh. Fiz.* **56** Issue 1 66
- [3] Koval N N, Kreindel Yu E, Schanin P M 1983 Generation of pulsed electron beams with uniform high current density distribution in systems with a grid plasma emitter *Zh. Tekh. Fiz.* **53** Issue 9 1846
- [4] Koval N N, Oks E M, Protasov Yu S, Semashko N N 2009 *Emission electronics* (Moscow, MGTU)
- [5] Gavrillov N V, Emlin D R, Kamenetskikh A S 2008 High-efficiency emission from a grid-stabilized plasma cathode *Zh. Tekh. Fiz.* **78**, Issue 10 59
- [6] Gavrillov N V, Kamenetskikh A S 2013 Self-oscillating mode of electron beam generation in a source with a grid plasma emitter *Zh. Tekh. Fiz.* **83** Issue 10 32
- [7] Devyatkov V N, Koval N N 2014 Effect of electron extraction from a grid plasma cathode on the generation of emission plasma *Journal of Physics: Conference Series* **552** 0102014.
- [8] Koval N N, Grigoryev S V, Devyatkov V N, Teresov A D, Schanin P M 2009 Effect of Intensified Emission During the Generation of a Submillisecond Low-Energy Electron Beam in a Plasma-Cathode Diode *IEEE Trans. Plasma Sci.* **37** 1890
- [9] Devyatkov V N, Koval N N and Schanin P M 2001 Generation of high-current low-energy electron beams in systems with plasma emitters *Rus. Phys. J.* **44** 9 937
- [10] Koval V, Lopatin V, Nguen Bao Hung and Ogorodnikov Alexander S. 2015 Low Pressure Discharge Characteristics in a Large Sized Hollow Cathode. Radiation and Nuclear Techniques in Material Science *Adv. Mater. Res.* **1084** 196
- [11] Korolev Y D, Frants O B, Landl N V, Shemyakin I A, Geyman V G 2013 High-Current Stages in a Low-Pressure Glow Discharge With Hollow Cathode *IEEE Trans. Plasma Sci.* **41**. 8. 2087
- [12] Grigoryev S V, Devyatkov V N, Koval N N, Teresov A D 2010 Enhanced Emission during Submillisecond Low Energy Electron Beam Generation in a Diode with Grid Stabilized Plasma Cathode and Open Anode Plasma Boundary *Tech. Phys. Lett.*, **36** 2 158
- [13] Grigoryev S V, Moskvina P V, Teresov A D 2012 Plasma emitter based on an asymmetric reflex discharge for a submillisecond electron beam *Proc. IV Intern. Kreindel Workshop on Plasma Emission Electronics (Ulan-Ude: Russia), June 25–30*, 112